*Hearing Research*, 21 (1986) 17–40
Elsevier



HRR 00673

# Directional hearing in the grassfrog (*Rana temporaria* L.). II. Acoustics and modelling of the auditory periphery

A.M.H.J. Aertsen [1,*], M.S.M.G. Vlaming [2], J.J. Eggermont [1,**] and P.I.M. Johannesma [1]

[1] *Department of Medical Physics and Biophysics, University of Nijmegen, Nijmegen, and*
[2] *Department of Applied Physics, Biophysics Group, Technical University Delft, Delft, The Netherlands*

(Received 16 April 1984; accepted after revision 2 October 1985)

In an earlier paper (Vlaming et al., 1984) we reported on optical measurements (laser-doppler interferometry) of the vibrations characteristics of the grassfrog's tympanic membrane. In the present paper these measurements were extended to include acoustic measurements concerning the functional role of the mouth cavity in frog hearing.

Based on these measurements a model of the frog's acoustic periphery, consisting of three coupled linear oscillators with three entrance ports for sound, was developed and analyzed mathematically to give the various relevant transfer functions. The model is characterized by six parameters, all of which could be estimated from the available experimental data. For frequencies up to some 1500 Hz the model adequately describes the experimental data, both our own and earlier, seemingly conflicting data in the literature. For higher frequencies deviations occur, possibly due to nonuniform vibrations of the membranes.

The model was used to evaluate the monaural directional sensitivity of the frog under free-field stimulation. Essentially it behaves as a combined pressure-gradient receiver, with highly frequency-dependent directional sensitivity. Directional sensitivity of the tympanic membrane could be modulated drastically by changing the resonance properties of the mouth cavity, without affecting the intrinsic membrane properties. This, theoretically, allows the frog to manipulate its direction sensitivity by actively tuning the volume of its mouth cavity. In order to account for discrepancies with known properties of low-frequency auditory nerve fibers an additional, extra-tympanic channel was included into the model. The extended model, the second-channel possibly involving the opercularis complex, provides a good quantitative fit to the available data on tympanic membrane movement as well as auditory nerve activity.

Finally, the model enables to simulate a (moving) sound source in space, while stimulating the frog via closed couplers.

directional hearing in frog, pressure-gradient receiver, model calculations, tympanic membrane vibrations, auditory midbrain

## Introduction

Classical mechanisms for directional hearing in birds and mammals are based on a simultaneous comparison of intensity, frequency spectrum, phase and time of arrival of the sound at the two ears. When interaural distances become smaller it is generally observed that the upper frequency limit of hearing increases, thereby providing sufficient head shadow effects and phase differences to maintain useful intensity or spectral differences (e.g. bats). In animals that rely predominantly on low-frequency hearing and have small interaural distance such as frogs and toads, differences in intensity and frequency spectrum between both ears become probably useless for localization of sound. However, at the upper frequency limit of hearing in the leopard frog (*Rana pipiens*) interaural intensity differences may still play a role (Feng, 1980). Furthermore in these cold-blooded animals from the temperate climatic regions, the minute interaural time differences for sound arrival at the two ears (cf. Table III) will be difficult to resolve. Moreover, at ambient temperatures of around 15°C the capability of the neural firings to phase lock with the stimulus ceases above around 300 Hz in

* *Present address*: Max-Planck-Institute for Biological Cybernetics, Spemannstrasse 38, D-7400 Tübingen, F.R.G.
** To whom reprint requests should be addressed.

the torus semicircularis of the grassfrog (Hermes et al., 1981), thus arguing against the use of the classical interaural phase-difference mechanism for localization.

Behavioral experiments (Rheinländer et al., 1979) have indicated that the tree frog *Hyla cinerea* is surprisingly accurate in localizing loudspeakers producing conspecific sounds or only sound at the dominant song frequency. The accuracy could be estimated at about 10°. Frogs use both ears for sound localization as has been demonstrated by Feng and Capranica (1976) and Rheinländer et al. (1979), thus some mechanism based on binaural hearing that is useful in sound localization at low frequencies must be available. The suggestion has been forwarded that a pressure gradient-sensitive system could produce the required localization accuracy (Strother, 1959; Chung et al., 1978; Rheinländer et al., 1979).

When we consider the eardrums which are internally coupled through the mouth cavity (Strother, 1959) to form asymmetric pressure gradient receivers (Fletcher and Thwaites, 1979a) then phase differences at the eardrums again may play an important role in the directional hearing of frogs. Pressure gradient receivers have an inherent directionality by their response which depends on phase differences across the membrane. This directionality, however, depends on the frequency of the sound in relation to the acoustics of the coupled ears.

It has been observed that directional hearing based on a pressure gradient mechanism is especially pronounced in the frequency range of the species song and this generally corresponds to a resonance of the tympanum displacement. This has been observed in the female cicada (*Cystosoma saundersii*) (Fletcher and Hill, 1978), the cricket (*Teleogryllus commodus*) (Fletcher and Thwaites, 1979b), the field cricket (*Gryllus campestris*) (Paton et al., 1977; Kleindienst et al., 1981), and the Japanese quail (Hill et al., 1980; Coles et al., 1980). Existing analog models of the coupled eardrums in the frog result in resonance frequencies for eardrum displacement which are dominated by the unloaded tympanum resonance but slightly modified by the added compliance of the mouth cavity (Fletcher and Thwaites, 1979a).

Experimental results led Chung et al. (1978) to suggest that all resonance was due to the resonating mouth cavity (resonance frequency 1750 Hz) at the upper end of the hearing range in grassfrogs (Brzoska et al., 1977).

According to the first model, opening the mouth cavity would effectively isolate both ears acoustically but the tympanum would still show a resonance. The results from Chung et al. (1978), however, would suggest that the eardrums are nearly unresponsive when the mouth is opened.

Moffat and Capranica (1978) using light scattering spectroscopy studied the response characteristics of the tympanum in various anurans using a closed sound system and found basically a low-pass characteristic. Chung et al. (1978, 1981) on the other hand found a band-pass or resonator type of response under free-field stimulation condition. These two sets of experiments have been repeated and both of them were confirmed by Pinder and Palmer (1983). In a previous paper (Vlaming et al., 1984) we repeated Moffat and Capranica's findings for closed sound system stimulation in the grassfrog.

Considering the ears as the only entrance ports for sound, pressure-gradient mechanisms would require considerable cross-talk between both eardrums through the eustachian tubes and mouth cavity. Strother (1959) already observed that obstructing the eustachian tubes gave losses up to 34 dB at the opposite ear; the same was reported by Feng and Capranica (1976). Chung et al. (1978) observed in the grassfrog at the resonance frequency (1750 Hz) a cross-talk of $-6$ dB measured in the vibration amplitude of the eardrum. Feng (1980) measured responses of single fibers from the auditory nerve in the leopard frog with respect to the direction of the sound source. He observed that the acoustic cross-talk under closed mouth conditions in the 900–1100 Hz region was only $-4$ dB, increasing toward $-30$ dB for lower and higher frequencies.

The spectrum of the mating call in the leopard frog is bimodal with a low frequency peak near 500 Hz and a higher frequency peak above 1000 Hz (Liff, 1969). In the grassfrog the dominant call frequency is around 500 Hz (Brzoska et al., 1977; Aertsen and Johannesma, 1980) with still some energy at 1100 and 1500 Hz, although about 20 dB lower than in the 500 Hz region. Thus, the leopard

frog and grassfrog are more or less comparable in this respect. The results of Feng (1980) therefore indicate that the best coupling between the eardrums is not at the dominant frequency in the calls. In addition, Aertsen and Johannesma (1980) have observed that the higher frequency components in the calls are predominantly found at the onset of the call elements. So there is still a possibility that only this part of the call serves localization and the main energy part together with the temporal structure has a more communicative meaning.

Feng (1980) observed for auditory nerve fibers with best excitatory frequencies below 400 Hz an angular variation dependence proportional to $\cos \theta$, i.e., figure-of-8 directionality curves. This points to a directionality as observed in a single membrane symmetrical pressure-gradient system requiring that the membrane is equally accessible from both sides. Rheinländer et al. (1981) measured monaural directional characteristics on basis of multi-unit thresholds in the torus semicircularis contralateral to the right ear after abolishing the neural input from the left inner ear. They reported a figure-of-8 response characteristic for a single eardrum (open mouth) in *Hyla cinerea,* which under closed-mouth conditions changed into the characteristic cardioid response pattern of an asymmetrical pressure gradient receiver (see also Feng and Shofner, 1981; Wilczynski et al., 1981).

We investigated the acoustic properties of the auditory periphery of the grassfrog both with laser-doppler interferometry (for a full report cf. Vlaming et al., 1984) and by pressure measurements in the mouth cavity under closed and free-field stimulation. In addition, we measured the response of the contralateral tympanum both with laser interferometry as well as by pressure built up in a closed system comparable to that described by Rosowski and Saunders (1980) and Kleindienst et al. (1981). The acoustic crosstalk was measured under mouth open and closed conditions.

On basis of these experimental data a model was designed that is capable of explaining the findings of Moffat and Capranica (1978), Chung et al. (1978, 1981), and, more recently, Pinder and Palmer (1983) and Vlaming et al. (1984). The model, which is a modification of the Fletcher and Thwaites model (1979a), essentially consists of three coupled linear oscillators with three entrance ports for sound. The observed band-pass behaviour of the single eardrum in free field (frontal stimulation) (Chung et al., 1978, 1981) is shown to be due to *interference* of the individual contributions in the model, each one with its particular directional characteristics (cf. Fig. 9). In addition, this model explains directional characteristics for a single tympanic membrane. Model predictions confronted with auditory nerve data from Feng (1980) conform in the mid- and high-frequency range; for low frequencies distinct discrepancies occur. In this context we discuss our model in comparison with other proposals (Pinder and Palmer, 1983, 1984) and postulate an alternative: the inclusion of a parallel, extra-tympanic channel, which is mainly effective in the low-frequency band and which might possibly involve the operecularis complex.

## Methods

Adult grassfrogs (*Rana temporaria* L.) from Ireland were anaesthetized using a 0.05% solution of MS-222. After disappearance of the cornea reflex the animal was placed in a sound-attenuated room (IAC type 120 A) in which temperature was kept near 15°C. This ensured that skin respiration was sufficient to maintain a good oxygen supply to the animal. The skull was fixed and a stimulation and monitoring system was attached to the head and surrounding the tympanic membranes, a probe microphone was entered into the mouth cavity.

Most experiments were performed in the initial phase of an experiment involving also electrophysiological recordings from the auditory midbrain. In a number of cases, after the frog recovered from the initial MS-222 anaesthesia the animal was injected with a muscle relaxant (Buscopan; for details see Eggermont, 1983a). As a result the acoustic measurements contain data on anaesthetized frogs and immobilized frogs, as well as a few cases where measurements were made during both stages.

Closed sound-system stimulation was performed using a specially designed coupler based on a Sennheiser (MD 211N) electrodynamic microphone, the details of which have been published previously (Hermes et al., 1981).

The microphone at the contra-lateral ear was constructed in an identical way: the housing was identical to the stimulating system with the exception that the driver system for the Sennheiser microphone was removed (Kleindienst, 1981; Rosowski and Saunders, 1980). The monitoring Brüel & Kjaer (type 4134) 1/2-inch condenser microphone stayed in its original position, thereby being coupled to the eardrum by a volume of 2.7 $cm^3$. The probe microphone in the mouth consisted of a Brüel & Kjaer (4134) 1/2-inch microphone and a standard coupling to a 2.5 cm long probe with an inner diameter of 1.3 mm.

As a stimulus a 2 ms duration gamma-envelope (Aertsen and Johannesma, 1980) -shaped electrical signal was delivered to the stimulator. The acoustic stimulus waveform was occasionally measured at the place of the tympanic membrane and all results obtained were corrected for the acoustic spectrum of the stimulus. Click intensity was at 89 dB peak-equivalent SPL. The output level of the condenser microphones was measured using a Brüel & Kjaer (type 2606) measuring amplifier and a type 2619 pre-amplifier. Clicks were presented at a rate of 13/s and responses were averaged (BIOMAC 1000) for 512 up to 4096 presentations depending on the strength of the response and read by a PDP 11/34. Power and phase spectra were calculated and corrected for stimulus and probe characteristics. Free-field stimuli were delivered using small loudspeakers, the sound waveforms were measured just outside the mouth cavity and inside the closed mouth cavity using the same probe microphone in both cases.

During free-field stimulation both ear-couplers were left in place, thereby effectively shielding the ears. Furthermore the nares were vaseline-sealed, thus excluding also these as possible pathway for sound to enter the mouth. In a number of cases additional measurements were made with the frog's head also immersed in water up to the level of the lower rim of the mouth.

## Experimental results

Measurements were made on 25 frogs. No systematic differences were observed between measurements from anaesthetized frogs and those from immobilized frogs. The measurements on acoustic crosstalk generally showed a sharp peak, with peak frequencies varying between 500 and 1300 Hz, mostly however lying around 900 Hz. The peak frequency generally was somewhat (in the order of 100 Hz) lower than the in-phase frequency ($\Delta\phi = 0$). No systematic differences were observed between left to right transmission and the opposite direction. The sound pressure level in the closed mouth upon one-sided stimulation using the closed sound system generally showed a broader peak, with peak frequency mostly equal to or somewhat higher (up to a few hundred Hz) than the crosstalk measurements. The in-phase frequency in these measurements generally was lower than the peak frequency; in fact, very often it was close to the peak frequency for cross-talk. Again no systematic differences were observed between left- and right-ear stimulation. Opening the mouth virtually abolished the sound pressure, measured in the mouth and, especially, in transmission.

Using free-field stimulation the general finding for the sound pressure in the closed mouth, di-

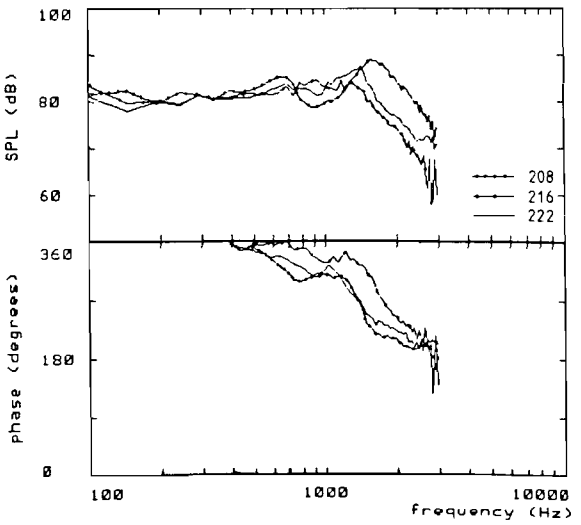


Fig. 1. Amplitude (top) and phase (bottom) of sound pressure level inside the closed mouth (eardrums fitted with couplers that shielded free field and nares vaseline-sealed) as a function of frequency, measured for three different frogs under free-field stimulus conditions. Sound pressure level refers to a level of 80 dB SPL, measured in the vicinity of the frog's head. For frequencies below 400 Hz the phase-curves have not been drawn because in this modulo-$2\pi$ picture the oscillations around 0° ( = 360°) would give rise to uninteresting excursions.

vided by the sound pressure just outside the mouth, was a curve showing two peaks, one between 500 and 900 Hz, the other, generally larger one between 1000 and 1600 Hz. For very low frequencies the ratio slowly decreased to one, the phase shift going to zero. It appeared that sound in the mouth cavity was generally not attenuated at all for frequencies below some 2000 Hz. A few typical examples are given in Fig. 1, showing sound pressure in the closed mouth, normalized to a level of 80 dB SPL just outside the mouth. It should be noted that these results were obtained with eardrums fitted with couplers that shielded free field and nares vaseline-sealed (see Methods). Furthermore, immersion in water up to the mouth's lower rim hardly changed the sound pressure in the mouth, suggesting that the pathway from outside to inside is not really localized, at least not in the areas just mentioned and that transparency for sound into the mouth cavity might well be a more general property distributed over the frog's entire head (see also Wilczynski et al., 1981, 1982).

For more detailed results on the tympanic membrane displacement and sound pressure in the mouth under various stimulus conditions we refer to our previous paper (Vlaming et al., 1984). The tympanic membrane results can be summarized as follows: At 80 dB SPL the ipsi ear-vibration amplitude in the low frequencies is about 30 nm rising to about 50 nm around 850 Hz and for frequencies above 900 Hz a typical roll off in the order of 12–18 dB/octave is found. The response amplitude of the contra-lateral ear shows in all but one ear a typical bandpass character: maximum transmission is around 900 Hz. Response amplitude at that frequency appears to be only 6 dB down with respect to the ipsilateral response.

## Model

*General formulation*

The experimental findings, both from optical measurements (Vlaming et al., 1984) and acoustical measurements (present paper), provide the necessary constraints for an attempt to model the frog's acoustic periphery. The model should be linear and has to show the demonstrated symmetry in response properties of both tympanic membranes. It should be an oscillator-type model with

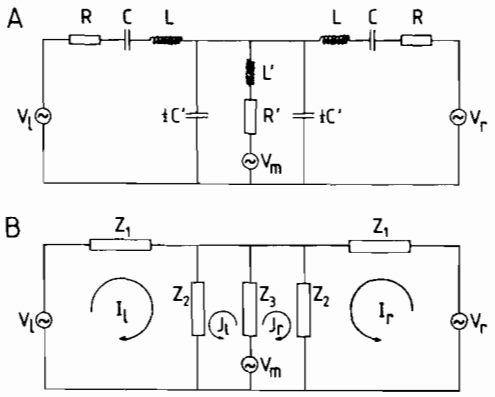


Fig. 2. Model of tympanic pathway in the acoustic periphery of the frog, adapted from Fletcher and Thwaites (1979a). Top: coupled RLC-oscillators, bottom: more abstract formulation, showing current loops used for derivation of maze equations. The three voltage sources ($V_l$, $V_m$, $V_r$) represent the entrance ports for sound, the currents ($I_l$, $I_r$) correspond to the volume velocities at the tympanic membranes. Further explanation in the text.

the appropriate resonance properties and coupling characteristics. Furthermore, in addition to sound pressure acting through the gate-ways of the tympanic membranes, it appeared that sound easily enters the closed mouth cavity (nares being shut), irrespective of the ears being sealed or not, giving rise to a model with three possible entrance ports for sound pressure.

In analogy to Fletcher and Thwaites (1979a) we decided to set up a model as shown in Fig. 2. In Fig. 2A the resonance properties of tympanic membranes and mouth cavity are modelled by coupled RLC oscillators, for symmetry reasons the capacitance representing mouth volume and elasticity is split up in two. Three driving forces represent the sound pressure acting under free-field conditions. A more abstract version of the model is shown in Fig. 2B, where the impedances are given by

$$Z_1 = R + i\omega L + \frac{1}{i\omega C} \tag{1a}$$

$$Z_2 = \frac{2}{i\omega C'} \tag{1b}$$

$$Z_3 = R' + i\omega L' \tag{1c}$$

with $i = \sqrt{-1}$

Using the indicated current loops we arrive at a formulation of the four maze equations

$$V_l = Z_1 I_l + Z_2(I_l + J_l) \tag{2a}$$

$$V_m = Z_2(I_l + J_l) + Z_3(J_l + J_r) \tag{2b}$$

$$V_m = Z_2(I_r + J_r) + Z_3(J_l + J_r) \tag{2c}$$

$$V_r = Z_1 I_r + Z_2(I_r + J_r) \tag{2d}$$

Defining a set of abbreviations (the $\eta$'s being admittances)

$$\eta_1 = \frac{1}{2Z_1} \tag{3a}$$

$$\eta_2 = \frac{1}{2(Z_1 + Z_2)} \tag{3b}$$

$$\eta_3 = \frac{Z_2^2}{2(Z_1 + Z_2)(Z_1 Z_2 + 2Z_1 Z_3 + 2Z_2 Z_3)} \tag{3c}$$

$$\eta_4 = \frac{Z_2}{Z_1 Z_2 + 2Z_1 Z_3 + 2Z_2 Z_3} \tag{3d}$$

$$\eta_5 = \frac{2(Z_1 + Z_2)}{Z_1 Z_2 + 2Z_1 Z_3 + 2Z_2 Z_3} \tag{3e}$$

which combine to

$$\alpha_1 = \eta_1 + \eta_2 + \eta_3 \tag{4a}$$

$$\alpha_2 = -\eta_1 + \eta_2 + \eta_3 \tag{4b}$$

$$\alpha_3 = -\eta_4 \tag{4c}$$

$$\alpha_4 = \eta_5 \tag{4d}$$

we arrive at the following transfer matrix

$$\begin{pmatrix} I_l \\ I_r \\ I_m \end{pmatrix} = \begin{pmatrix} \alpha_1 & \alpha_2 & \alpha_3 \\ \alpha_2 & \alpha_1 & \alpha_3 \\ \alpha_3 & \alpha_3 & \alpha_4 \end{pmatrix} \begin{pmatrix} V_l \\ V_r \\ V_m \end{pmatrix} \tag{5}$$

where $I_m = J_l + J_r$ represents the net 'mouth-current'.

Taking into account that in this electric analogy the current represents volume velocity and voltage represents sound pressure, then charge in turn will represent volume displacement (Olson, 1958). Thus Eqn. (5) describes the frequency domain relations between the various sound pressure inputs and the resulting volume velocity outputs of the linear system in Fig. 2. By virtue of the electric analogy it follows that velocity ratios will be identical to the corresponding displacement ratios, when stated in frequency terms. It may be noted how the symmetry of the acoustic periphery is reflected in the symmetry of the transfer matrix. Another quantity of experimental interest, the sound pressure level *within* the closed mouth $U_m$ can be found from Eqn. (5) by using

$$U_m = V_m - I_m Z_3 \tag{6}$$

In the following we will consider in some more detail the characteristics of the model under specific stimulus conditions as reported in the experimental sections.

*Closed sound system, one-sided stimulation*

This case can be described by having $V_l \neq 0$ and $V_m = V_r = 0$. Here it has been assumed that the external load, $Z_e$ provided by the volume of the air cavity between the tympanic membrane and the microphone used for measuring the sound pressure at the contralateral ear (see Methods) is negligible compared to the impedance $Z_1$ of the membrane. The coupler volume (2.7 $cm^3$, see Methods) corresponds to a capacitance of approximately $2 \times 10^{-11}$ $kg^{-1}$ $m^4$ $s^2$; comparison to the estimated values for the eardrum capacitance which are in the order of $1 \times 10^{-12}$ $kg^{-1}$ $m^4$ $s^2$ (cf. Table I) shows that the eardrum impedance is about twenty times larger than the impedance added by the external load, thus we infer that indeed $V_m = V_r = 0$ is a fair approximation. Moreover, it has been assumed that the attachment of the couplers per se does not alter the impedance $Z_1$ of the membranes themselves. This obviously is a fundamental assumption when comparing results from free-field vs. closed sound system (coupler) measurements.

As a measure for interaural tympanic membrane coupling we study the ratio $q$ of contralateral and ipsilateral membrane displacement (cf. Fig. 7 in Vlaming et al., 1984). Due to the

circular symmetry of the membranes this equals the ratio of volume displacements (here: charge $Q$), each of which in turn equals the corresponding volume velocity (here: current $I$), divided by $i\omega$. Thus we have

$$q = \frac{Q_c}{Q_i} = \frac{I_c}{I_i} \tag{7}$$

where the subscripts i and c denote ipsi- and contralaterally, respectively. For ipsilateral stimulation we get from Eqn. (5) for the coupling $q$

$$q = \frac{\alpha_2}{\alpha_1}$$

which, upon substitution of the 'abbreviations' (3) and (4), leads to

$$q = \frac{-Z_2 Z_3}{Z_1 Z_2 + 2Z_1 Z_3 + Z_2 Z_3} \tag{8}$$

Substitution of the original variables in terms of $R$, $L$ and $C$, using Eqn. (1), and some elaboration leads to

$$q^{-1} = -1 - \frac{Z_1}{R'} \cdot A(\omega) \tag{9a}$$

where

$$A(\omega) = \frac{1 + i\left(\frac{\omega^3}{\omega_0'^3} Q_3' - \frac{\omega}{\omega_0'} Q_3' + \frac{\omega}{\omega_0'} \frac{1}{Q_3'}\right)}{1 + \left(\frac{\omega}{\omega_0'} Q_3'\right)^2} \tag{9b}$$

$$\text{where } \omega_0' = (L'C')^{-1/2} \tag{10a}$$

is the undamped resonance frequency

$$\text{and } Q_3' = \omega_0' \frac{L'}{R'} \tag{10b}$$

is the quality factor.

From Eqns. (9a, b) it follows that the coupling $q$ (more appropriate, its inverse $q^{-1}$) as determined under ipsilateral stimulus conditions, deviates from $-1$ to an amount which is equal to the product of (a) the ratio of ear impedance $Z_1$ and mouth damping $R'$, and (b) a frequency dependent term which only contains the mouth's filter characteristics: undamped resonance frequency $\omega_0'$ and quality factor $Q_3'$.

By analogous reasoning it follows for the ratio $u_1$ of sound pressure *in* the closed mouth $U_m$ relative to the driving pressure at the eardrum $V_1$

$$u_1 = \frac{U_m}{V_1} = \frac{Z_2 Z_3}{Z_1 Z_2 + 2Z_1 Z_3 + 2Z_2 Z_3} \tag{11}$$

Combination of the results for $q$ and $u_1$ (Eqns. 8, 11) leads to the following reciprocal relations

$$u_1 = \frac{q}{q - 1} \tag{12a}$$

$$q = \frac{u_1}{u_1 - 1} \tag{12b}$$

emphasizing the equivalence of information obtained from laser measurement of tympanic membrane displacement ratio, as a measure for interaural coupling, and acoustic measurement of sound pressure in the closed mouth cavity, i.e. the coupler between the two ears.

*Free-field stimulation, both ears closed*

In this case the only driving force is $V_m \neq 0$; we may set $V_1 = V_r = 0$. As in the previous case, the effect of the external load on the frog's acoustic system, imposed by attaching the acoustic couplers, will be neglected. The most important quantity, at the same time experimentally relatively easily accessible, is the sound pressure level *within* the closed mouth, caused by sound entering the acoustic system by whatever pathway from the outside to the inside, with the obvious exception of the closed-off ears and the vaseline-sealed nares.

After substitution of the relevant voltage values into Eqn. (5) and some elaboration we obtain for the ratio of inside and outside sound pressure level

$$u_m = \frac{U_m}{V_m} = \frac{Z_1 Z_2}{Z_1 Z_2 + 2Z_1 Z_3 + 2Z_2 Z_3} \tag{13}$$

It now may be instructive to carry through the substitution to the level of $R$, $L$, $C$ variables,

using Eqns. (1a–c), which leads to

$$u_m(\omega) = \left(1 - \omega^2 L'C' + i\omega R'C' + 2i\omega R'C \cdot \frac{1 + i\omega \frac{L'}{R'}}{1 - \omega^2 LC + i\omega RC}\right)^{-1} \quad (14)$$

Closer inspection of Eqn. (14) indicates that, qualitatively speaking, the behaviour of $u_m(\omega)$ can be described by the simple resonance curve of the isolated mouth oscillator, this resonance curve, however, being 'excavated' over a certain region and to an extent determined principally by (1) the uncoupled tympanic membrane resonance curve and (2) the quality of the mouth oscillator, (3) mediated by the $R'C$-coupling of both oscillators. This 'excavation' may give rise to two pseudo-peaks, surrounding the trough (cf. Fig. 1). Clearly this modified resonance-type build-up of sound pressure in the closed mouth cavity under natural free field conditions will contribute to the ultimate tympanic membrane displacement. This contribution, from Eqn. (14), will largely be determined by the relative tuning and quality characteristics of the separate resonators involved.

*Parameter estimation*

The general case of natural free-field conditions will be a linear combination of the separate influences described in the foregoing, the quantitative formulation is given in Eqn. (5). In order to assess the relative importance of the various terms we will have to make reasonable estimations regarding the possible values of the six parameters involved: the components $R$, $L$, $C$ and $R'$, $L'$, $C'$, respectively.

*1. Tympanic membrane: R, L, C.* The tympanic membrane parameters are the ones most easily and accurately obtainable. This is realized if we observe the displacement curve of the ipsilateral membrane with closed-system stimulation and open mouth, as measured in the laser-doppler experiment (cf. Fig. 3 in Vlaming et al., 1984). Since an open mouth corresponds to $C'$ going to infinity, effectively shunting both the mouth and the contralateral ear, we are left with the 'pure' ipsilateral ear oscillator (cf. Fig. 2A).

From the open-mouth ipsilateral curve of Rana 209 (cf. Vlaming et al., 1984), which we use as a typical example, we obtain the following approximate figures:

- Static membrane displacement $x(0) \simeq 32$ nm at pressure $p = 80$ dB SPL $= 0.2$ Pa.
- Damped amplitude resonance $x(\omega_A) \simeq 67$ nm at approximately 850 Hz: $\omega_A \simeq 2\pi \cdot 850\ s^{-1}$.
- For the quality $Q_3$, defined by

$$Q_3 = \omega_0 \frac{L}{R} \quad (15)$$

with the undamped resonance frequency $\omega_0$ defined by

$$\omega_0^2 = \frac{1}{LC} \quad (16)$$

we obtain, by using the relation

$$\frac{x(\omega_A)}{x(0)} = Q_3 \left(1 - \frac{1}{4Q_3^2}\right)^{-1/2} \quad (17)$$

the estimate value $Q_3 \simeq 2.18$. In Eqn. (17) it has been assumed that the membrane as a whole moves in phase and that the profile does not change with frequency. Actual measurements of the membrane movement (Vlaming et al., 1984) show that both assumptions are justified for frequencies below some 1000–1400 Hz.

- The damped amplitude resonance frequency relates to the undamped frequency as

$$\left(\frac{\omega_A}{\omega_0}\right)^2 = 1 - \frac{1}{2Q_3^2} \quad (18)$$

Substitution of the estimates for $\omega_A$ and $Q_3$ leads to $\omega_0 \simeq 2\pi \cdot 900\ s^{-1}$.

If we assume the tympanic membrane to be circular with radius $r$ (Rana 209: $r \simeq 1.5$ mm) and furthermore assume the static membrane displacement profile to be parabolic and radially symmetric, we obtain from the static displacement, by

using

$$C = \frac{\pi r^2 x_0}{2p} \tag{19}$$

an estimate for the ear's compliance

$$C \simeq 5.60 \times 10^{-13}\ \mathrm{kg^{-1}\ m^4\ s^2}$$

This estimate is not drastically altered by using an estimate for the actual volume displacement based on the experimentally determined membrane profile (cf. Fig. 5 in Vlaming et al., 1984). Combination of the above given figures and relations then gives the estimates for the remaining parameters:

$$R \simeq 1.45 \times 10^{8}\ \mathrm{kg\ m^{-4}\ s^{-1}}$$

$$L = 5.60 \times 10^{4}\ \mathrm{kg\ m^{-4}}$$

Analogous reasoning applied to the other three frogs for which tympanic membrane data are available led to the estimations listed in Table I. The first three columns give the values for the parameters $R$, $L$ and $C$, the remaining two present the associated filter characteristics: undamped resonance frequency $\omega_0/2\pi$ and quality $Q_3$ as a measure for bandwidth. Because of the small sample size and the lack of an underlying model of the distribution of these parameters over a reasonably sized frog population we will continue working with the individual estimates, rather than resort to some arbitrary type of average measure.

*2. Mouth cavity: R', L', C'.* The parameters characterizing the coupling between both ears, lumped into the mouth cavity oscillator, can be obtained relatively easily from measurements of the sound pressure build-up in the closed mouth during one-sided stimulation with a closed sound system (cf. Eqn. 11). In order to be able to relate the results to the ear parameters given above we will again use the experimental data from Vlaming et al. (1984), i.e. their Figs. 9 (directly measured values of $U_m$) and 10 (corrected for probe effects).

The theoretical expression for the ratio $u_1 = U_m/V_1$ in this case is given by Eqn. (11). It can be shown that the asymptotic behaviour of this ratio, for low- and high-frequency stimulation is given by

$$u_1(\omega) \simeq i\omega R'C \quad (\text{for } \omega \to 0) \tag{20a}$$

$$u_1(\omega) \simeq -\frac{1}{\omega^2 LC'} \quad (\text{for } \omega \to \infty) \tag{20b}$$

This relatively simple asymptotic frequency dependence of $u_1(\omega)$ thus predicts low- and high-frequency slopes of $|u_1(\omega)|$ of $+6$ and $-12$ dB/octave, respectively, and phase angles approaching 90° and 180°, all of which is fairly corroborated by the experimental findings in Figs. 10 and 9b from Vlaming et al. (1984). Using the earlier determined values for the ear parameters $L$ and $C$, an estimate can be derived for the mouth parameters $R'$ and $C'$ by fitting the simplified expressions (20a, b) to the experimental curves. This fit was performed simply by hand, the results are listed in Table II. With 5 of the 6 parameters now known, the remaining one, $L'$, can be estimated from a particular point of the $u_1(\omega)$ curve. For this point we choose the undamped ear reso-

TABLE I

ESTIMATES OF EAR-PARAMETERS AND ASSOCIATED FILTER CHARACTERISTICS, DETERMINED FROM OPTICAL MEASUREMENTS OF TYMPANIC MEMBRANE DISPLACEMENT UNDER CLOSED SYSTEM STIMULATION AND OPEN MOUTH

From Vlaming et al. (1984). Further explanation in text.

| Rana | $R$ (kg m$^{-4}$ s$^{-1}$) | $L$ (kg m$^{-4}$) | $C$ (kg$^{-1}$ m$^4$ s$^2$) | $\omega_0/2\pi$ (Hz) | $Q_3$ |
|---|---|---|---|---|---|
| 205 | $8.86\times10^{7}$ | $5.75\times10^{4}$ | $1.57\times10^{-12}$ | 530 | 2.16 |
| 206 | $8.65\times10^{7}$ | $3.27\times10^{4}$ | $1.0\ \times10^{-12}$ | 880 | 2.09 |
| 207 | $9.52\times10^{7}$ | $3.96\times10^{4}$ | $1.0\ \times10^{-12}$ | 800 | 2.09 |
| 209 | $1.45\times10^{8}$ | $5.60\times10^{4}$ | $5.60\times10^{-13}$ | 900 | 2.18 |

TABLE II

ESTIMATES OF MOUTH PARAMETERS AND ASSOCIATED FILTER CHARACTERISTICS, DETERMINED FROM MEASUREMENT OF SOUND PRESSURE IN CLOSED MOUTH CAVITY UPON ONE-SIDED STIMULATION OF THE EAR, USING A CLOSED SOUND SYSTEM

From Vlaming et al. (1984). Further explanation in text.

| Rana | $R$ (kg m$^{-4}$ s$^{-1}$) | $L'$ (kg m$^{-4}$) | $C'$ (kg$^{-1}$ m$^4$ s$^2$) | $\omega_0/2\pi$ (Hz) | $Q_3'$ |
|---|---|---|---|---|---|
| 206 | $1.0 \times 10^7$ | $3.27 \times 10^3$ | $7.75 \times 10^{-12}$ | 1000 | 2.05 |
| 207 | $3.18 \times 10^7$ | $2.76 \times 10^3$ | $2.55 \times 10^{-12}$ | 1900 | 1.05 |
| 209 | $1.79 \times 10^7$ | $7.25 \times 10^3$ | $3.59 \times 10^{-12}$ | 990 | 2.51 |

nance $\omega_0$ because it is in between the low- and high-frequency regions, already used for estimating $R'$ and $C'$; furthermore, it facilitates the actual calculation by eliminating certain terms. The resulting expression for $L'$ becomes

$$L' = \frac{iR'}{\omega_0} + \frac{iR}{\omega_0} \cdot \left( 2 - \frac{1}{u_1(\omega_0)} + i\omega_0 RC' \right)^{-1} \qquad (21)$$

Substitution of the various numerical values leads to the estimates of $L'$ listed in Table II, which also contains the estimated filter characteristics of the mouth oscillator ($\omega_0'/2\pi$ and $Q_3'$) for the three frogs for which data are available.

## Model results

*Reconstruction of optical and acoustical measurements*

Before addressing the question of directional sensitivity we will have to make sure that the model is consistent with the experimental data on tympanic membrane displacement and sound pressure in the mouth under the artificial stimulus conditions as described.

The results for one-sided closed coupler stimulation, mouth being shut ($V_l = 1$, $V_r = V_m = 0$), are given in Figs. 3–6. These results, like the other ones in this section, were obtained using the parameter values listed in Tables I and II. In each case the top half of the figure gives the amplitude spectrum on log scale, the lower half gives the phase spectrum on linear scale; (the horizontal) frequency axis is always logarithmically. Fig. 3 shows the displacement of the ipsilateral tympanic membrane, the contralateral membrane is given in Fig. 4.

The absolute scaling from charge-units (integrated current) to displacement in nm was obtained by using Eqn. (19). All results in this section refer to a stimulus level of 80 dB SPL (0.2 Pa). The coupling between the membranes, as expressed in the ratio of contralateral and ipsilateral displacement (Fig. 4 'divided by' Fig. 3) is given in Fig. 5. Finally the sound pressure level in the

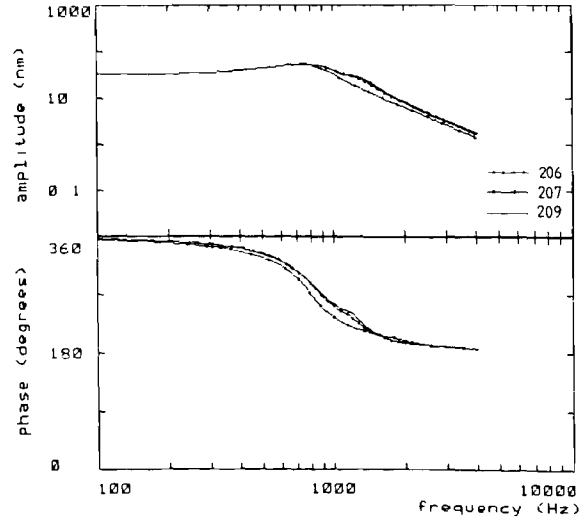


Fig. 3. Model calculations of displacement amplitude (top) and phase (bottom) of the centre of the tympanic membrane as a function of stimulus frequency for ipsilateral closed coupler stimulation at 80 dB SPL (mouth closed). The three curves correspond to different parameter values, estimated for as many different frogs, using optical and acoustic data from Fig. 2 of Vlaming et al. (1984); the numbers refer to the identification used there.

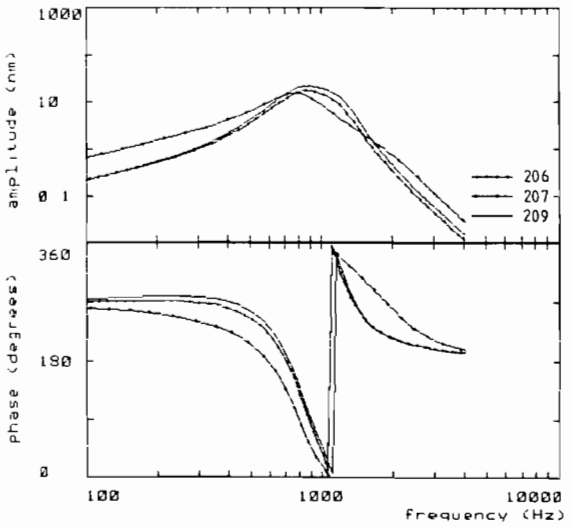


Fig. 4. As Fig. 3, now for contralateral stimulation. Compare to Fig. 6 of Vlaming et al. (1984).

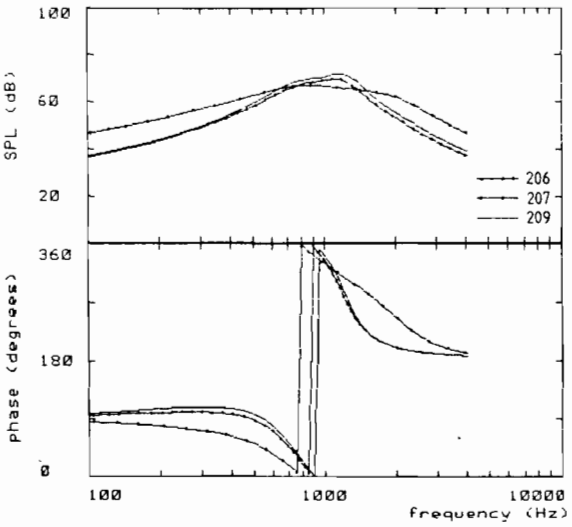


Fig. 6. Model calculations of amplitude (top) and phase (bottom) of sound pressure level in the closed mouth for closed coupler stimulation at one ear. Further details as in Fig. 3. Compare to Figs. 9 and 10 of Vlaming et al. (1984).

mouth cavity is shown in Fig. 6. These model results should be compared to the actual measurements given by Vlaming et al. (1984) as shown in their Figs. 2, 6, 7 and 9/10, respectively (see also Moffat and Capranica, 1978). This comparison shows that for frequencies below some 1500 Hz the model results in Figs. 3–6 indeed closely follow the measured results, both for the amplitude and phase characteristics. For higher frequencies we note marked discrepancies in the behaviour of especially the contralateral membrane (and consequently the ratio) and, to a lesser degree, the sound level in the mouth. These differences are characterized by an additional secondary amplitude peak around 2 kHz and a persistent fast half-phase rotation (ipsi- and contra membrane) and a local counter rotation around 2 kHz (sound level in mouth), as opposed to the predicted gradual amplitude decline and phase approaching the asymptotic value of 180°. This result is consistent with the observation of Vlaming et al. (1984) that for frequencies below 1000–1400 Hz the movement of the membrane is uniform, whereas for higher frequencies deviations become apparent, especially in the region where the columella is attached. In the present model we have used uniformity of vibration of the whole membrane as a basic assumption.

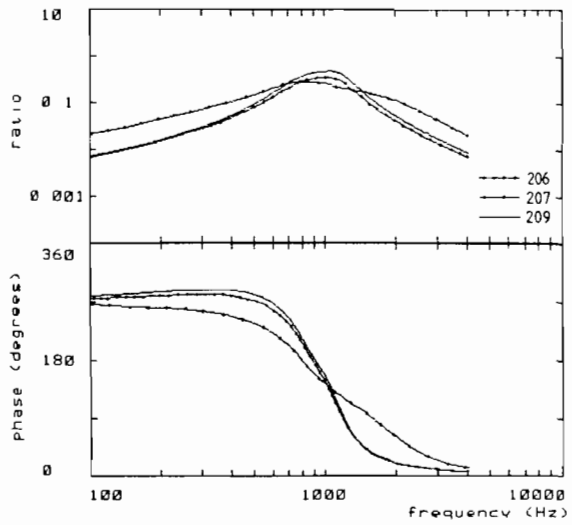


Fig. 5. Model calculations of ratio of displacement amplitude (top) and phase shift (bottom) for contralateral and ipsilateral coupler stimulation (Fig. 4 'divided by' Fig. 3). Compare to Fig. 7 of Vlaming et al. (1984).

On the whole the results for Rana 207 show a less satisfactory consistency between model calculations and actual measurements than the other two frogs. We ascribe this reduced performance to a possible less accurate estimation of the mouth

parameters, due to more dominant high frequency deviations from uniformity as reflected in the sound level measurements in the closed mouth, used for estimating $C'$ and, indirectly $L'$ (Fig. 10 of Vlaming et al., 1984).

The results for free field stimulation, both ears shielded from free field and nares sealed ($V_m = 1$, $V_l = V_r = 0$) are shown in Figs. 7 and 8. Fig. 7 gives the displacement for the tympanic membrane, which for reasons of symmetry is the same for both ears now. Fig. 8 shows the sound pressure level in the closed mouth. Measurements to test the consistency of Fig. 7 are not available. The theoretical results in Fig. 8 may qualitatively be compared to the measurements as given in Fig. 1, although it should be noted that the theoretical curves again correspond to the parameter values from Tables I and II, whereas the measurements in Fig. 1 were made on other frog individuals. Comparing Figs. 1 and 8 we indeed note a close correspondence between the model results using the parameters for Ranas 206 and 209 with the measurements from Rana 208. This correspondence holds for both the amplitude and phase. The model result for Rana 207 deviates significantly, presumably for the reasons indicated earlier. It is

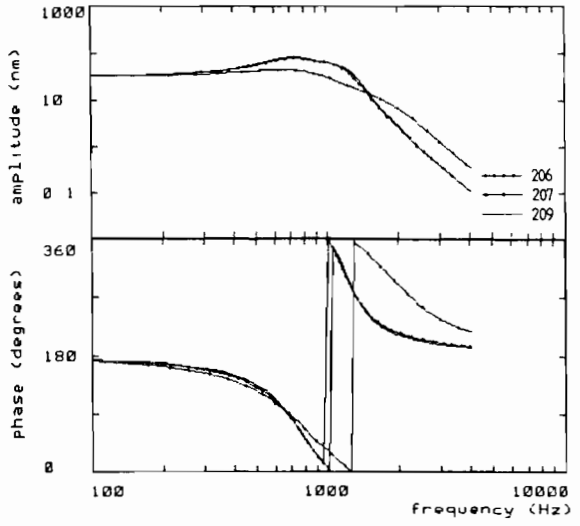


Fig. 7. Model calculations of displacement (top) and phase (bottom) of the centre of the tympanic membrane under free-field stimulation (80 dB SPL just outside the head, mouth closed, both ears shielded from direct stimulation). Further details as in Fig. 3.

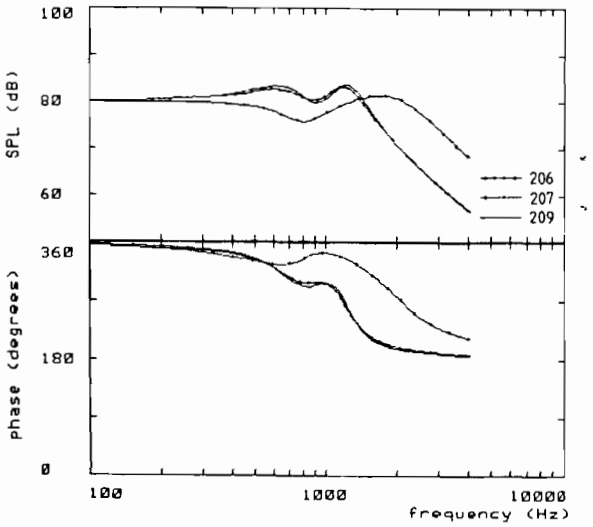


Fig. 8. Model calculations of amplitude (top) and phase (bottom) of sound pressure level in the closed mouth under free-field stimulation (80 dB SPL just outside the head, both ears sealed). Further details as in Fig. 3. Compare to Fig. 1.

of further interest to note that the curves for Ranas 206, 209 and 208 correspond to frogs having their ear- and mouth-oscillator tuned to the same frequency (900–1000 Hz), whereas the measurements for Ranas 216 and 222 indicate a higher frequency tuning of the mouth oscillator (about 1400 and 1200 Hz), with no change, however, in the tuning of the ear oscillator. We will return to this point later. With respect to Fig. 7 we note the large displacement amplitude, especially for frequencies below some 1500 Hz, comparable to or even stronger than in the case of ipsi-stimulation (cf. Fig. 3), however, with a phaseshift between the two varying between 180° (low frequency) and almost 90° (around 1500 Hz). Indeed, we should expect strong interference effects for the membrane displacements due to the two pathways for sound compared here.

Summarizing, the comparison between model results and experimental data under different stimulus conditions indicates that the model given in Fig. 2 with the estimated parameters as given in Tables I and II truly is consistent, at least for frequencies up to some 1500 Hz, which encompasses most of the frequency range relevant for hearing in this particular species. For frequencies above 1500 Hz we have noted discrepancies, prob-

ably due to the experimentally observed non-uniform vibration behaviour of the tympanic membranes, a fact which is not taken into account in the present model. Based on these results we now proceed with somewhat more confidence to the behaviour under physiologically more relevant stimulus conditions (i.e. free field) and the question of directional sensitivity.

*Model calculations for free-field conditions: directional sensitivity of the single ear*

In the case of free-field stimulation we have the full model, described by Eqn. (5), with sound entering through all three ports V. We assume the amplitudes of the three driving forces to be equal, due to the short distance between the ears and the lack of significant head-shadow. There will however be a phase shift between the V's, due to the slight delays in sound arrival, depending on the azimuth angle of sound incidence. We have treated the third entry port $V_m$ as being at the midpoint between the two ears, unlike Fletcher and Thwaites (1979a), who placed it forward of the tympana. The reason for this is that while in Fletcher and Thwaites (1979a) $V_m$ corresponds to the inlet through the nares, our measurements suggest that the third pathway from outside to inside is not really localized in e.g. the nares but instead is more a general property distributed over the frog's entire head (see Experimental results). Therefore we have associated $V_m$ with the 'center' of the head, thus losing frontal-backward directionality (Fletcher and Thwaites, 1979a), which leads to the following 'symmetrical' relations

$$V_l(t) = p(t-\tau)$$
$$V_m(t) = p(t) \qquad (22)$$
$$V_r(t) = p(t+\tau)$$

with $p(t)$ the sound pressure in the vicinity of the head, in between the two ears and $\tau$ the delay, given by

$$\tau = \frac{l \sin\theta}{c} \qquad (23)$$

with $2l$ the distance between the ears, $\theta$ the angle of sound incidence (frontal: $\theta = 0°$) and $c$ the velocity of sound, the transfer properties of the model are calculated in the frequency domain by having

$$V_l(\omega) = V_m(\omega)\, e^{-i\omega\tau}$$
$$V_r(\omega) = V_m(\omega)\, e^{+i\omega\tau} \qquad (24)$$

TABLE III

AZIMUTH ANGLES OF SOUND INCIDENCE AND CORRESPONDING DELAYS IN ARRIVAL TIMES, USED FOR CALCULATION OF DIRECTION-DEPENDENT TYMPANIC MEMBRANE DISPLACEMENT

| $\theta$ (°) | $\tau$ ($\mu$s) | $\theta$ (°) | $\tau$ ($\mu$s) |
|---|---|---|---|
| 0 | 0 | 40 | 18.91 |
| 5 | 2.56 | 45 | 20.80 |
| 10 | 5.11 | 50 | 22.53 |
| 15 | 7.61 | 60 | 25.47 |
| 20 | 10.06 | 70 | 27.64 |
| 22.5 | 11.26 | 80 | 28.96 |
| 30 | 14.71 | 90 | 29.41 |

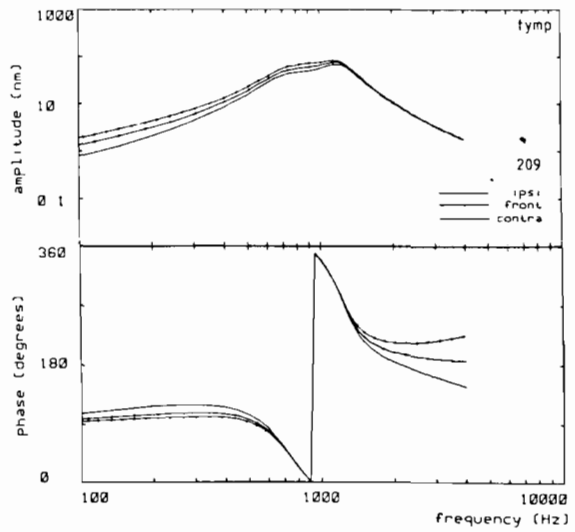


Fig. 9. Model calculations of displacement amplitude (top) and phase (bottom) of the centre of the tympanic membrane as a function of stimulus frequency under free field stimulation at 80 dB SPL, for three different azimuth angles of sound incidence ($-90°$, $0°$, $+90°$). Calculations were based on one set of parameter estimates as used in the foregoing figures (Rana 209, corresponding to a membrane resonance $f_0$ of 900 Hz and a mouth cavity resonance $f_0'$ of 990 Hz).

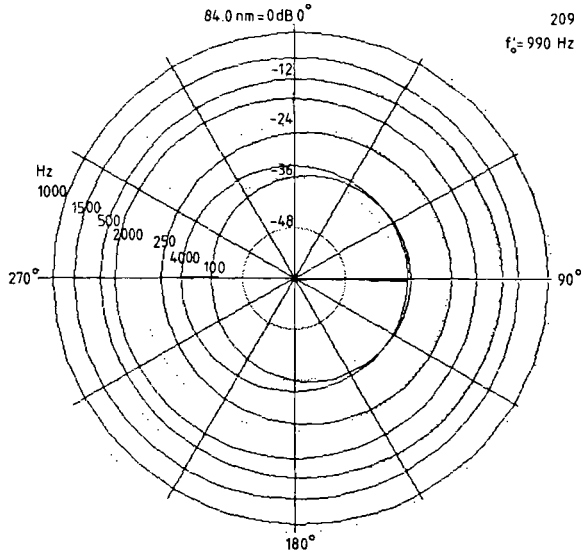


Fig. 10. Polar plot of model calculations of displacement amplitude of the centre of the tympanic membrane under free-field stimulation at 80 dB SPL, as a function of azimuth angle of sound incidence. Different curves represent different stimulus frequencies. Parameter values used were the same as in Fig. 9. The amplitude axis is in dB, with 0 dB referring to 84 nm, the maximum displacement amplitude throughout the range of frequencies and angles considered.

We have calculated the displacement of both tympanic membranes for various values of $\theta$, listed in the left column of Table III. Using the values of $l = 1$ cm and $c = 340$ m/s, this corresponds to the delays $\tau$ listed in the right column of Table III. For reasons of left-right symmetry it suffices to have only positive values of $\theta$, furthermore we have assumed complete front-back symmetry (cf. Eqn. 23), which restricts the relevant range of $\theta$ to the first quadrant. We have used the parameters of Rana 209 as a typical example. The results are shown in Figs. 9 and 10. Fig. 9 shows the calculated amplitude- and phase characteristics of the tympanic membrane displacement as a function of frequency for a sound stimulus of 80 dB SPL coming from three extreme directions: $-90°$, $0°$ and $+90°$, corresponding to, if we consider the right ear, completely contralateral, frontal and ipsilateral, respectively. The first obvious observation to be made is that now, contrary to the case of closed system stimulation, the membrane displacement shows a clear bandpass behaviour, irrespective of the angle of incidence. This evidently is the result of the interference of the three inputs from Eqn. (5), where especially in the low frequency region an almost complete cancellation occurs, as was to be expected from the comparison of the results in Figs. 3 and 7. This result from our model calculations thus indicates that the apparent discrepancy between the results from Moffat and Capranica (1978) and those from Chung et al. (1978) are explained by the difference in stimulation: closed system vs. free field. In the free-field situation the displacement due to sound directly acting on the membrane from the outside and the displacement due to sound entering into the mouth cavity ($V_m$) cancel at low frequencies, giving rise to a net displacement which behaves like a bandpass filter. The displacement due to the third pathway (via membrane to mouth to the inner surface of the membrane) appears to play a minor role here.

It is furthermore observed that largest displacements are found close to 1200 Hz, clearly above the membrane and mouth resonances, the displacement being in phase with the stimulus. At those frequencies, however, the ear is not very directionally sensitive: the amplitudes are virtually identical for the three angles considered. For lower frequencies we note a gradually increasing amplitude difference (less conspicuous for the phase), representing directional sensitivity, however, at the expense of a decreasing absolute sensitivity. At the lowest frequency tested (100 Hz) the difference in relative displacement between $-90°$ and $+90°$ amounts to about 8 dB, with an absolute value around only 1.3 nm. At 500 Hz, where much of the energy in the species-specific vocalizations is concentrated (e.g. Aertsen and Johannesma, 1980) the relative difference between extreme left and right still is about 3 dB, now, however, at an appreciable absolute displacement of almost 20 nm. Finally, at frequencies above 1 kHz we note complete overlapping of amplitudes and increasing phase differences. It is however, hard to imagine how the latter could ever be resolved by the frog brain which already in the periphery ceases to show phase locking above some 300 Hz (e.g. Hermes et al., 1981).

A better overall impression of directional sensitivity is obtained by plotting the displacement as a function of azimuth angle in a polar graph. Fig. 10 shows the results for the right ear, the scale is in

dB where 0 dB corresponds to 84.0 nm, the maximum amplitude throughout the observed frequency and azimuth range for a stimulus level of 80 dB SPL. Each curve represents one particular frequency. The directional sensitivity at low frequencies, which shows a monotonic dependence on the azimuth angle, now is apparent in the asymmetry of the polar plots, a feature which is altogether missing for high frequencies.

Summarizing, the model for the single ear predicts that going from low ($\approx$ 100 Hz) to higher (1000–1200 Hz) frequencies there is a trade-off between directional sensitivity (high at low frequencies) and absolute sensitivity (high around 1000 Hz), whereas for frequencies above 1200 Hz both decline rapidly.

*Effects of tuning the mouth oscillator*

It has been suggested (Rheinländer et al., 1981) that the frog, by varying its interaural pathway has the means to actively influence its directional sensitivity. This suggestion, combined with the experimental findings shown in Fig. 1, indicating

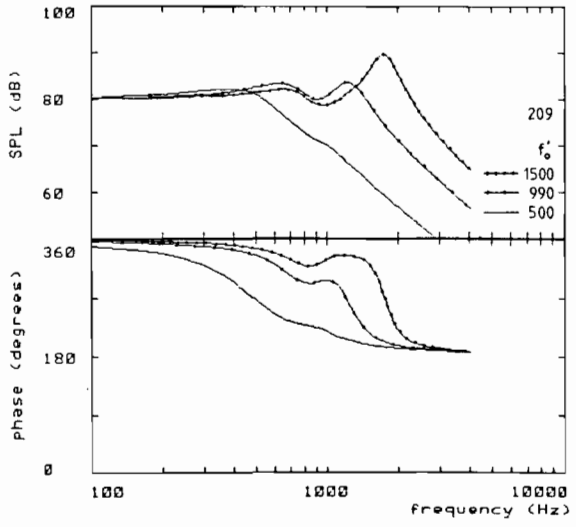


Fig. 11. Effect of tuning the mouth cavity: model calculations of amplitude (top) and phase (bottom) of sound pressure level in the closed mouth under free-field stimulation (80 dB SPL just outside the head, both ears shielded). Different curves represent different resonance frequencies $f_0'$ of the mouth cavity, obtained by changing the mouth capacity $C'$. Further parameter values as in the foregoing figures (Rana 209). Compare to Fig. 1.

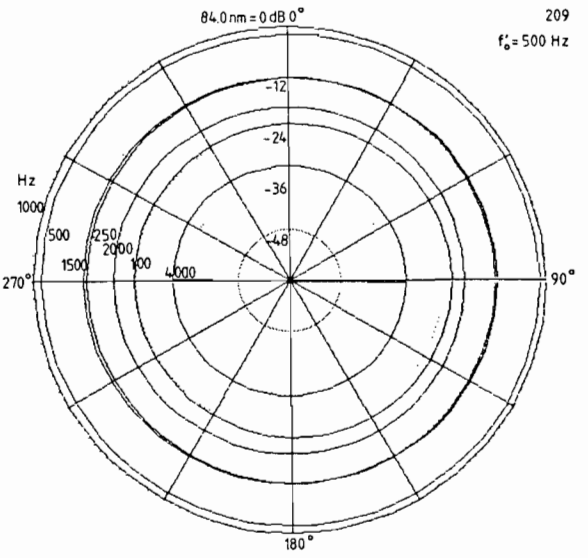


Fig. 12. Directional sensitivity of displacement amplitude as in Fig. 10, now for mouth cavity resonance $f_0'$ of 500 Hz.

that indeed the mouth oscillator can show tuning to frequencies differing appreciably from the tympanic membrane resonance of about 900 Hz, led us to investigate the possible relevance of variable mouth-oscillator tuning for directional hearing. To this end we have calculated the

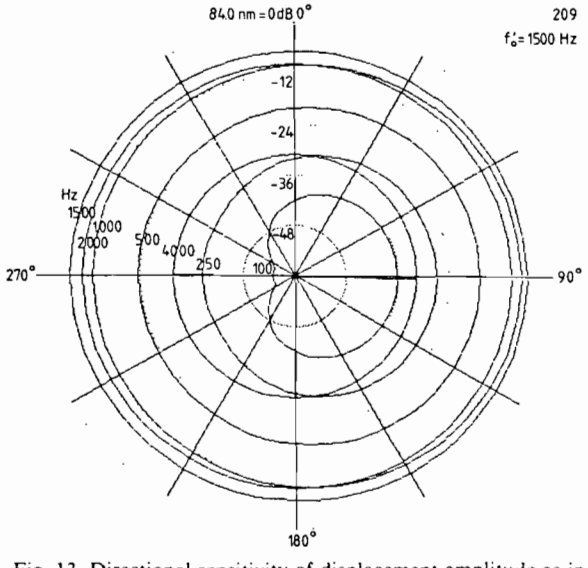


Fig. 13. Directional sensitivity of displacement amplitude as in Fig. 10, now for mouth cavity resonance $f_0'$ of 1500 Hz.

tympanic membrane displacement for different values of the mouth resonance frequency $f_0'$: 500, 990 and 1500 Hz. The case of 990 Hz simply is the case of Rana 209 used in the previous Figures, the other two frequencies were obtained by varying the mouth capacity $C'$ ($\approx$ mouth volume), keeping the other parameters at the original R209 values (500 Hz: $C' = 1.40 \times 10^{-11}$ kg$^{-1}$ m$^4$ s$^2$; 1500 Hz: $C' = 1.55 \times 10^{-12}$ kg$^{-1}$ m$^4$ s$^2$). These particular frequencies were chosen because 500 Hz corresponds to the frequency where the bulk of the energy in the species-specific vocalizations is concentrated ('croak-mouth') while 1500 Hz is at the upper end of the frequency scale and more or less mimics the experimental findings for Ranas 216 and 222 (cf. Fig. 1).

Fig. 11 shows the sound pressure level in the closed mouth upon free field stimulation, ears being shielded from direct sound incidence ($V_m = 1$, $V_l = V_r = 0$), for each of the three mouth resonances considered. This plot should be compared to the experimental results in Fig. 1. Apart from the earlier noted similarity between the 990 Hz curve (= R209) and R208 we observe the fair agreement between the 1500 Hz curve and R216, both in amplitude and phase behaviour. The 500 Hz curve is not present in our small sample of experimental data.

For each of the two mouth-variants we have calculated the tympanic membrane displacement as a function of azimuth-angle, for different stimulus frequencies as in Fig. 10. The results for the croak-mouth ($f_0' = 500$ Hz) are given in Fig. 12; Fig. 13 represents the case of a 1500 Hz mouth resonance. Results have been normalized to an absolute displacement of 84 nm at 80 dB SPL, the same value as used for R209, so that comparisons can be made. In the case of the low-frequency mouth we observe a clearly increased displacement at frequencies below 1000 Hz (cf. Fig. 12), at the expense, however, of directional sensitivity which stays well below the neural threshold of 2 dB for all frequencies and angles considered and below 1 dB if we only consider frequencies of 500 Hz and higher. For frequencies of 1000 Hz and higher both the absolute and directional sensitivity are hardly affected by tuning the mouth to 500 Hz. Quite the contrary observations can be made with regard to the 1500 Hz mouth (Fig. 13). In this case the displacement is reduced for frequencies of 1000 Hz and lower, whereas above 1000 Hz we note an increase in absolute sensitivity. The directional sensitivity shows a marked increase for all frequencies, the emphasis again on low frequencies. Note also the characteristic cardioid-type response for low frequencies in Fig. 13. It should be stressed, finally, that we have obtained here a marked shift in the net frequency sensitivity of the tympanic membrane, simply by manipulating the tuning of the mouth oscillator, without having to change the properties of the membrane oscillator itself whatsoever.

Based on these calculations we predict that Rana 216 (cf. Fig. 1), due to its higher tuned mouth, has increased directional sensitivity of tympanic membrane displacement, at the expense of low-frequency absolute sensitivity, whereas a frog that has its mouth tuning lowered to the croak frequency has increased absolute sensitivity, paying for that with a clearly reduced directional sensitivity. Summarizing, these model calculations show that indeed, as suggested by Rheinländer et al. (1981), the frog, by changing the volume of its mouth cavity, in principle has the capacity to influence the directional sensitivity of its tympanic membrane displacement. Whether this capacity is actively used during phonotaxis cannot be answered here; this should be the subject of further behavioural investigations (see also Rheinländer et al., 1981).

*Comparison to auditory nerve directional response curves*

The model presented here, with the parameters estimated from the results of various optical experiments, is able to 'explain' all measured tympanic membrane responses. Under free-field stimulation it provides a directional sensitivity of the membrane displacement which is frequency dependent: for decreasing frequency there is a monotonic increase in sensitivity for angle of sound incidence, apparent in the increasing ovoidal, or even cardioid-like appearance of the polar diagrams (cf. Figs. 10, 12 and 13).

This result would predict for all auditory nerve fibers to have sigmoidal directional response curves, the angle dependence more or less distinct, depending on frequency. For mid- and high-

frequency units (500–900 and 1200–2100 Hz, resp.) in the VIIIth nerve of *Rana pipiens* this is in accordance with the findings of Feng (1980), both qualitatively and quantitatively. For low-frequency units ($< 400$ Hz), however, the neural response curves have a V shape, the minimum falling within some 30° of the midline. This would correspond to a figure-8 directional sensitivity of the tympanic membrane, clearly not in accordance with the model predictions. Also from tympanic membrane displacement measurements there is no evidence for a figure-8 directional sensitivity at low frequencies. The stimulation thresholds reported by Feng (1980) for units with best frequencies of 170 Hz and 1900 Hz were quite comparable (51 and 45 dB SPL resp.), the model predicts a considerably larger difference between low- and mid- to high-frequency tympanic membrane displacement (Fig. 10: 15–30 dB, depending on precise frequencies considered). Actual measurements of tympanic membrane displacement (Pinder and Palmer, 1983; Vlaming et al., 1984) show comparable differences between low- and mid-/high-frequency displacement amplitudes.

Palmer and Pinder, in a recently published paper (1984), discuss a modified version of their earlier model (1983), the modification explicitly designed to cover also the V-shaped directionality of low-frequency auditory nerve fibers. Their model, basically also a Fletcher and Thwaites-type coupled oscillator model with three sound entrance ports, differs from our model (Fig. 2) mainly in one aspect: the inclusion of a frequency-dependent radiation resistance in the three sound pathways. By virtue of the $\omega^2$ proportionality of this radiation-resistance the model behaves quite differently for low and higher frequencies, and indeed gives rise to a figure-8 directionality at low-frequency and an ovoidal characteristic at higher frequencies. As a matter of fact, the two auditory nerve response curves presented by Feng (1980) can quite adequately be predicted, as far as their shape is concerned.

We have used the Palmer–Pinder model to calculate tympanic membrane response curves and beak SPL curves for different stimulus conditions, analogously to the curves presented earlier in this paper. Examples are given in Figs. 14 and 15, which show the predicted tympanic membrane displacement (Fig. 14) and sound pressure level in the closed mouth (Fig. 15) upon free-field stimulation, with both ears shielded from direction stimulation (compare our Figs. 7 and 8). For the

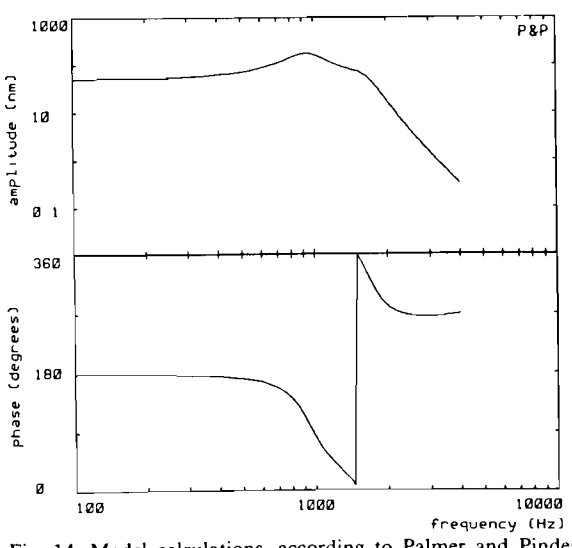


Fig. 14. Model calculations, according to Palmer and Pinder (1984), of displacement amplitude (top) and phase (bottom) of the centre of the tympanic membrane under free-field stimulation (80 dB SPL just outside the head, mouth closed, both ears shielded from direct stimulation). Compare to Fig. 7.

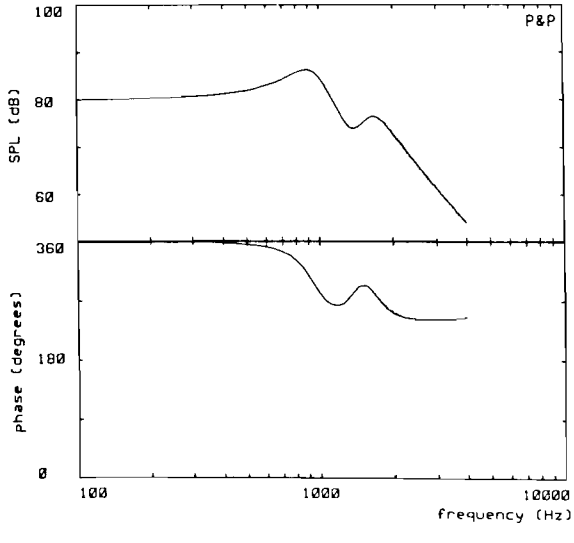


Fig. 15. Model calculations, according to Palmer and Pinder (1984), of amplitude (top) and phase (bottom) of sound pressure level in the closed mouth under free-field stimulation (80 dB SPL just outside the head, both ears sealed). Compare to Figs. 1 and 8.

model parameters we have used the values given by Palmer and Pinder (1984), except for the radiation resistance, where the proportionality factor 0.02 N $s^3$ $m^{-5}$ gave rise to inconsistent results (apparently a misprint) and we have used instead the value of 7.54, reconstructed from their original formulation of the model (Pinder and Palmer, 1983). In the latter case we were able to reconstruct their polar plots of directional dependence of membrane displacement. From these curves we noted that, although the shapes of the curves match Feng's auditory nerve curves surprisingly well, there is a distinct difference in amplitude: the 170 Hz curve is more than 30 dB down with respect to the 1900 Hz curve, which is hard to reconcile with the auditory nerve thresholds given by Feng. Observation of the various tympanic membrane and beak SPL curves (e.g. Figs. 14 and 15) showed that in general the amplitude curves were very comparable to the curves predicted by our model, however, that distinct differences appeared for the phase curves. Comparison of Figs. 7 and 14 resp. 8 and 15, for example, shows that for high frequencies both the tympanic membrane movement and the beak-SPL according to Palmer and Pinder should approach a phase lag with respect to the stimulus of some 90°, whereas our model would predict a phase difference of 180° in both cases. Comparison with actual measurements (beak-SPL: Fig. 1; tymp. membrane: Figs. 3, 11 in Vlaming et al., 1984) suggests that a 180° phase shift for high frequency sound entering the closed mouth provides a better fit to the data. Similar differences can be observed for ipsilateral stimulation, now for frequencies approaching zero. Again the experimental evidence is rather more in favour of the curves predicted by our current model. Finally, the use of an $\omega^2$-dependent resistance in the Palmer and Pinder model (1984, 1983), which is essential there to obtain the low-frequency V-shaped directionality, in our view is not quite convincing. This resistance is introduced as the 'acoustic radiation resistance' of tube-like structures (eustachian tubes and nare tubes). Later in the development of the model the nare tubes have to be shifted to the interaural plane, which also in Palmer and Pinder (1984) is suggested to be a 'somewhat bizarre anatomical arrangement'. Furthermore our observations on the third entrance port suggest that transparency for sound into the mouth cavity is rather an overall property of the entire frog's head, eliminating the necessity for tube-like structures there altogether (see also Eggermont, 1986).

Summarizing, we have the following, rather confusing situation: (1) our current model (Fig. 2) which is able to explain all measured tympanic membrane displacement data and sound measurements inside the closed mouth; with correct predictions of mid- and high-frequency directionality of auditory nerve fibers but failing to explain the low-frequency neural directionality (both in shape and amplitude); (2) the modified Palmer–Pinder model (1984), which is clearly superior with respect to predicting also the figure-8 shape of neural direction sensitivity for low frequencies, but with a quite dramatic underestimation of the absolute sensitivity in that domain; furthermore with problems regarding the phase behaviour of certain acoustic and optic measurements and, finally, the necessity of a strongly frequency dependent resistance for not quite convincing reasons (see also Eggermont, 1986); and (3) an apparent discrepancy between the magnitude of low-frequency tympanic membrane movement (Pinder and Palmer, 1983; Vlaming et al., 1984) and auditory nerve thresholds (Feng, 1980), a similar discrepancy can be observed in neural audiograms measured from multi-unit recordings in the torus semicircularis (Brzoska et al., 1977; Eggermont, 1986): below some 500 Hz the tympanic membrane displacement is at least 10 dB too small to explain the neural thresholds.

*Modified model: additional extra-tympanic low-frequency channel*

In view of the foregoing we assert that there is no necessity to change our model (Fig. 2) as far as tympanic membrane movement is concerned: Eqns. (1–5), together with the estimated parameters, provide a fully adequate description of all known experimental data on tympanic membrane displacement and beak-SPL under various stimulus conditions, including free field.

At the same time the noted discrepancies with the neural data suggest that tympanic membrane displacement is *not* the only link between air-borne sounds and neural activity in the frog's auditory nervous system. This is in accordance with earlier

papers (e.g. Chung et al., 1981; Wilczynski et al., 1982), which stressed the existence of an extra-tympanic acoustic pathway to the inner ear fluids, which should be mainly effective for low-frequency sound (below 300–400 Hz). This extra-tympanic pathway, possibly involving the opercular complex, has been investigated in more detail by Lombard and colleagues (Hetherington and Lombard, 1982; Lombard and Straughan, 1974; Lombard et al., 1981) a recent review can be found in Eggermont (1986).

Based on these ideas we put forward the hypothesis that in order to explain the activity in the auditory nerve, our tympanic membrane model should be supplemented with a parallel, extra-tympanic system acting on the inner ear fluids. This additional system obviously should be 'invisible' for measurement of the tympanic membrane movement. Our suggestion for this second system is depicted in Fig. 16; it consists of two coupled RLC oscillators with three entrance ports for sound, in a symmetrical arrangement. Each oscillator is driven by the interference of sound passing through two entrance points: one at the lateral side and one in the middle. The attenuation through both channels is assumed equal, and is lumped into the oscillators. This arrangement is a typical example of a (double) pressure-gradient receiver and leads to a figure-8 directional characteristic. The required properties of the oscillators are dictated by the earlier discussed discrepancies between tympanic membrane displacement and auditory nerve activity: a low-frequency resonance ($\approx 200$ Hz), moderate filter quality ($Q_3 \approx 1$) and absolute sensitivity such that it matches the measured low-frequency auditory nerve thresholds. These specifications are reasonably met by the following set of parameters:

$$R'' = 1.5 \times 10^{8} \text{ kg m}^{-4} \text{ s}^{-1}$$

$$L'' = 1.2 \times 10^{5} \text{ kg m}^{-4}$$

$$C'' = 5 \times 10^{-12} \text{ kg}^{-1} \text{ m}^{4} \text{ s}^{2}$$

In view of the rather crude level of modelling and lacking more quantitative data on the extra-tympanic sound channel, no further attempts were undertaken to optimize the parameter values, let alone 'explain' them on structural or physiological grounds: the additional model is a purely functional model in the sense that it attempts to describe quantitatively the required performance of the second channel, necessary to close the low-

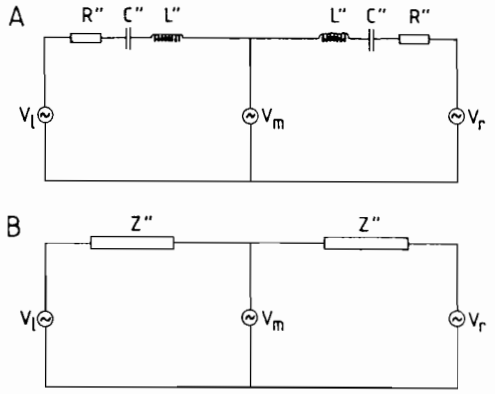


Fig. 16. Model of extra-tympanic pathway in the acoustic periphery of the frog. Top: RLC oscillators, bottom: impedance representation. The three voltage sources ($V_l$, $V_m$, $V_r$) represent the entrance ports for sound, identical to those in Fig. 2. Further explanation in text.

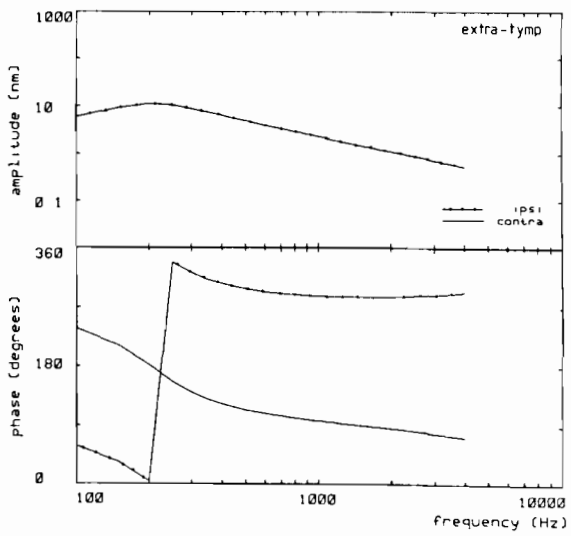


Fig. 17. Model calculations of contribution from extra-tympanic pathway to effective inner-ear stimulation under free-field stimulation at 80 dB SPL, expressed as *equivalent* tympanic membrane displacement amplitude (top) and phase (bottom) as a function of frequency. Curves are shown for ipsilateral and contralateral sound incidence.

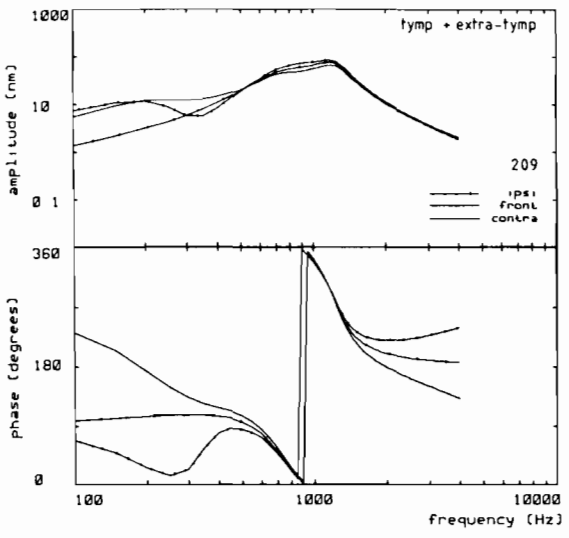


Fig. 18. Model calculations of effective inner-ear stimulation, expressed as *equivalent* tympanic membrane displacement amplitude (top) and phase (bottom) as a function of frequency, under free-field stimulation (80 dB SPL). The effective inner-ear stimulation is calculated as the sum of contributions from tympanic pathway (cf. Fig. 9) and extra-tympanic pathway (cf. Fig. 17). Curves are shown for three different azimuth angles of sound incidence ($-90°$, $0°$, $90°$).

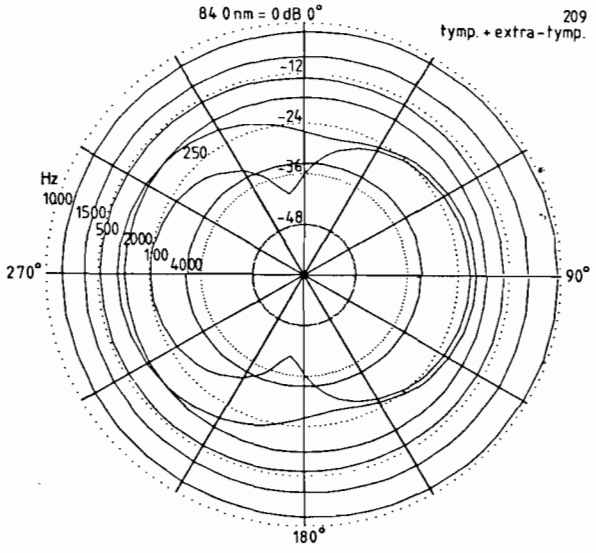


Fig. 19. Polar plot of model calculations of effective inner ear stimulation, expressed as *equivalent* tympanic membrane displacement amplitude (cf. Fig. 18) under free-field stimulation at 80 dB SPL, as a function of azimuth angle of sound incidence. Further details as in Fig. 10.

frequency gap between eardrums displacement and auditory nerve activity.

The additional stimulation of the inner ear due to this extra-tympanic channel is limited to the amphibian papilla and is graphically shown in Fig. 17: amplitude (upper trace) and phase (lower trace) for two free-field stimulus conditions: ipsilateral and contralateral. The graphs express the inner ear stimulation in terms of *equivalent* tympanic membrane displacement (in electrical analogy terms: charge), not to be confused with real membrane displacements. As is to be expected from the nature of the model, the ipsi- and contralateral response differs only in their phase behaviour: a frequency-independent shift of 180°. The curve for frontal stimulation is not shown, being identical to zero. Curves for intermediate angles show intermediate behaviour.

The net stimulation of the inner ear is obtained by summation of the contributions from the tympanic channel (cf. Fig. 9) and the extra-tympanic channel (Fig. 17). The result for three extreme angles of sound source localization (ipsi, front, contra) is shown in Fig. 18, again expressed in *equivalent* eardrum displacement. The frontal curves in Figs. 9 and 18 are identical; the ipsi and contra curves indeed show the low-frequency enhancement, required to match the auditory nerve threshold data; for mid and high frequencies the summation results (Fig. 18) are hardly discernible from the purely tympanic membrane results (Fig. 9). The directional sensitivity of the summated model is shown in polar coordinates for different frequencies in Fig. 19. This result should be compared to the purely tympanic result in Fig. 10, normalization being the same in both cases. For mid- and high frequencies both polar plots show the same, more or less ovoidal directionality; for low frequency we now obtain the distinct sign of a pressure-gradient receiver, resulting in a V-shape direction sensitivity of the auditory nerve with reasonable absolute sensitivity. It is interesting to note that the angle of minimum response does not coincide with the midline, a result which is not obtained by having nare-like structures displaced from the ear-to-ear line (as in Fletcher and Thwaites, 1979a; Palmer and Pinder, 1984; Pinder and Palmer, 1983), but simply reflecting the relative magnitudes of the contributions from tympanic

(ovoidal) and extra-tympanic (symmetric figure-8) channels. Due to the phase behaviour of both contributions the least preferred angle furthermore proves to be frequency dependent (in Fig. 19: some 10° left at 100 Hz, some 10° right for 250 Hz). In this context it is interesting to note that in his data on low-frequency units in the right auditory nerve, Feng (1980) observed that least preferred directions were distributed within some 30° on *either* side of the midline; there is no indication of a possible frequency dependence in his data as is suggested by our curves (see also Fig. 18).

Summarizing, we conclude that the inclusion into our tympanic model of a parallel extra-tympanic channel of the type presented here quantitatively solves the earlier discussed problems regarding low-frequency auditory nerve units without impairing in any way the already attained level of explanation of tympanic membrane movement and mid- and high-frequency nerve data. The ultimate test for a model of this sort obviously lies in quantitative measurements on the involvement of operculum and columella in the process of sound transduction as a function of frequency and angle of sound incidence.

**Discussion**

In an earlier paper (Vlaming et al., 1984) we presented experimental data on the vibration properties of the frog's tympanic membrane under various stimulus conditions. Both in that paper and in the present one we also investigated the role of the mouth cavity by measuring the sound pressure in the cavity under closed coupler stimulation as well as free-field stimulation with sealed ears and nares. Based on these experimental findings we developed a model for the frog's acoustic periphery. The model, the structure of which follows an earlier idea from Fletcher and Thwaites (1979a), essentially consists of three coupled RLC oscillators, corresponding to the two ears, coupled by the mouth cavity and the eustachian tubes. The model has three effective sound entrance ports: the two eardrums and some pathway from the outside to the mouth cavity, not involving the ears and nares. The model has been analyzed to give an explicit formulation of the relevant transfer functions. Using the experimentally corroborated symmetry of the ears, the model contains six parameters which we have been able to estimate from the experimental data.

Calculations based on these estimates showed a good agreement between theoretical results and the various measurements for frequencies up to some 1500 Hz. Furthermore, it proved possible to reconcile the earlier published and seemingly contradictory measurements on tympanic membrane displacement using closed coupler stimulation (Moffat and Capranica, 1978) and free-field stimulation (Chung et al., 1981, 1978). The model explains these discrepancies from the differences in stimulation, affecting the membrane through different entrance ports. In an elegant series of experiments Pinder and Palmer (1983) recently arrived at the same conclusion. For frequencies above 1500 Hz our model calculations deviated significantly from the measurements. This may be attributed to the experimentally found higher order vibration modes in that frequency regime (Vlaming et al., 1984), whereas the model assumes uniform vibration irrespective of frequency.

Fletcher and Thwaites (1979a), and following them Pinder and Palmer (1983), discussed a very similar model for the frog's ear, in which they considered as the three effective sound entrances the two eardrums and the nares. Our experiments on sound entering the cavity indicate that the third pathway, although it may involve the nares, is certainly not confined to them, and may rather be a more distributed property of the frog's head (Wilczynski et al., 1981, 1982). Furthermore, those authors arbitrarily select the membrane resonance $f_0$ at 1500 Hz, i.e. close to the net peak sensitivity of the membrane in free field, to be in accordance with the results from Chung et al. (1978). Our measurements (Vlaming et al., 1984), however, indicate that the membrane oscillator itself is tuned rather to lower frequencies (about 900 Hz). Even in the case of coincident tuning of membrane and mouth cavity around 900 Hz the interaction of the three oscillators will cause the net peak sensitivity of the membrane to shift to higher frequencies (around 1200 Hz). Moreover, our calculations suggest that the measured relatively high-frequency bandpass behaviour of the membrane in free field can well be accounted for solely by an upward shift of the mouth tuning, i.e. decreasing its volume,

as was indeed measured in a number of cases, rather than shifting the eardrum resonances themselves to values not encountered in our (limited) set of experiments, which would furthermore seriously affect the absolute sensitivity below 1000 Hz, the most interesting frequency band for frog communication.

We have used the model to evaluate the theoretical directional sensitivity of the single frog ear. At low frequencies the two membranes behave as uncoupled pressure gradient receivers, due to the interference of sound acting directly on the outer surface of the membrane and the pressure on the inner surface resulting from sound entering the mouth cavity through the relatively sound-transparent head. At high frequencies we have the familiar mammal-like configuration of two uncoupled pressure receivers. At intermediate frequencies (around 900–1000 Hz), corresponding to the resonance frequency of the isolated membrane oscillator (Vlaming et al., 1984) the membranes behave as coupled pressure–pressure gradient receivers, due to the additional effect of strong interaural coupling in that frequency regime. Summarizing: the present model of the frog's ear behaves as a combined pressure–pressure gradient receiver, the directional sensitivity being highly frequency-dependent, as was originally suggested by Feng and Shofner (1981).

The directional sensitivity of the tympanic membrane could further be improved by tuning the mouth oscillator to a higher resonance frequency, not affecting the membrane's own resonance, however, at the expense of absolute sensitivity at low frequencies. Such a shift in mouth tuning was indeed found in a number of our experimental animals (also Pinder and Palmer (1983) report a wide range of what essentially are mouth best frequencies); however, whether this property of the model actually corresponds to an actively used mechanism is beyond the scope of the present paper. Shifting the mouth tuning to low frequencies, i.e. tuning it to the main frequency of the species-specific vocalizations, leads to the converse: deterioration of directional sensitivity with an increase in absolute sensitivity at low frequencies. Again, the possible significance of this property awaits further behavioural experiments.

The model of tympanic membrane movement was supplemented with a parallel, extra-tympanic channel to account for discrepancies with data on low-frequency auditory nerve fibers (Feng, 1980). In our view the inclusion of an additional channel provides not only an adequate quantitative explanation of the available acoustic and neural data, but is also preferable above alternatives (Palmer and Pinder, 1984; Pinder and Palmer, 1983), e.g. in that it takes into account earlier ideas about the possible involvement of the operecularis complex in sound transduction (Hetherington and Lombard, 1982; Lombard et al., 1981; Eggermont, 1986). So far the second channel has only been incorporated as a 'missing term'; the reasoning about its form and quantitative aspects remains at a purely curve-fitting type level. Regarding the structural and physiological argumentation one might proceed along the ideas expressed by Hetherington and Lombard (1982): "It is hypothesized that at such resonance frequencies the middle ear cavity pulsates to such an extent as to produce auditory stimulation without requiring the tympanum–stapes pathway. Stimulation would occur rather through a shaking of the entire otic capsule produced by the pulsations of the adjacent middle ear cavity". As can be seen from Fig. 16, our version of the second channel would require that stimulation of the inner ear would involve two driving forces, one at the side and one in the middle, to obtain the necessary pressure gradient character. In how far involvement of the operecularis complex and relative sound transparency of e.g. tympanum for the one entrance port and distributed sound transparency of the head together with the influence of the mouth cavity for the middle entrance port would underlie the form of the hypothetized sound channel remains subject to more specific investigation.

The predicted strong frequency dependence of the direction sensitivity, poses interesting questions regarding the possible interrelations between tonotopy and spatial maps as organizational principles in the auditory midbrain, especially if we include the mouth coupling as a possible additional variable. Rather than having two separable 'axes' of organization and, consequently, of signal analysis in the brain, this would suggest a strong interdependence of space and frequency in the neural representation of sound, a possibility

which for instance might lead to a less orderly representation when only one variable is considered in isolation. Up to the present date the reports on both tonotopy and spatial organization as separate organizations in the frog's auditory midbrain have not been overwhelming. The possibility of intrinsically coupled spatio-spectro-temporal receptive fields as processing units has only tentatively been treated, more or less in passing (Aertsen and Johannesma, 1981; Eggermont et al., 1983b).

Finally, the present model, provided that more experimental results become available to give some insight into the distribution of the various parameters involved, will enable us to calculate the way in which closed sound stimulation of both ears can be conducted in a way to more or less mimic faithfully a (moving) sound source in space, thereby avoiding the numerous experimental difficulties associated with true free-field experiments.

## Acknowledgements

This investigation was supported by the Netherlands Organization for the Advancement of Pure Research (ZWO). Calculations were performed using the MATFUN software package developed at the Department of Medical Physics and Biophysics at the University of Nijmegen. The authors are grateful for skilful software support by Jan Bruijns and Wim van Deelen, for critical reading of the manuscript by Willem Epping and to Marianne Nieuwenhuizen and Janice Henry who prepared the manuscript. Part of this project was carried out while the first author (A.A.) was a visiting research fellow, first at the Max-Planck-Institut für biologische Kybernetik in Tübingen (F.R.G.) with Valentino Braitenberg, and later with George Gerstein at the Department of Physiology, University of Pennsylvania School of Medicine in Philadelphia (U.S.A.).

## References

Aertsen, A.M.H.J. and Johannesma, P.I.M. (1980): Spectro-temporal receptive fields of auditory neurons in the grass-frog. I. Characterization of tonal and natural stimuli. Biol. Cybern. 38, 223–234.

Aertsen, A.M.H.J. and Johannesma, P.I.M. (1981): The spectro-temporal receptive field. A functional characteristic of auditory neurons. Biol. Cybern. 42, 133–143.

Brzoska, J., Walkowiak, W. and Schneider, H. (1977): Acoustic communication in the grass frog (*R. temporaria*): calls, auditory thresholds and behavioral responses. J. Comp. Physiol. 118, 173–186.

Chung, S.H., Pettigrew, A. and Anson, M. (1978): Dynamics of the amphibian middle ear. Nature 272, 142–147.

Chung, S.H., Pettigrew, A.G. and Anson, M. (1981): Hearing in the frog: dynamics of the middle ear. Proc. R. Soc. London Ser. B 212, 459–485.

Coles, R.B., Lewis, D.B., Hill, K.G., Hutchings, M.E. and Gower, D.M. (1980): Directional hearing in the Japanese quail (*Coturnix c. japonica*) II. Cochlear physiology. J. Exp. Biol. 86, 153–170.

Eggermont, J.J. (1986): Physiological mechanisms of sound localization in anura. In: The Evolution of the Amphibian Auditory System. Editors: B. Fritzsch, T. Hetherington, M. Ryan, W. Walkowiak and W. Wilczynski. Wiley and Sons, Chichester (in press).

Eggermont, J.J., Epping, W.J.M. and Aertsen, A.M.H.J. (1983a): Stimulus dependent neural correlations in the auditory midbrain of the grassfrog (*Rana temporaria* L.). Biol. Cybern. 47, 103–117.

Eggermont, J.J., Epping, W.J.M. and Aertsen, A.M.H.J. (1983b): Binaural hearing and neural interaction. In: Hearing – Physiological Bases and Psychophysics, pp. 237–243. Editors: R. Klinke and R. Hartmann. Springer-Verlag, Berlin.

Feng, A.S. (1980): Directional characteristics of the acoustic receiver of the leopard frog (*Rana pipiens*): A study of the eighth nerve auditory responses. J. Acoust. Soc. Am. 68, 1107–1114.

Feng, A.S. and Capranica, R.R. (1976): Sound localization in anurans I. Evidence of binaural interaction in dorsal medullary nucleus of bullfrogs (*Rana catesbeiana*). J. Neurophysiol. 39, 871–881.

Feng, A.S. and Shofner, W.P. (1981): Peripheral basis of sound localization in anurans. Acoustic properties of the frog's ear. Hearing Res. 5, 201–216.

Fletcher, N.H. and Hill, K.G. (1978): Acoustics of sound production and of hearing in the bladder cicada *Cystosoma saundersii* (Westwood). J. Exp. Biol. 72, 43–55.

Fletcher, N.H. and Thwaites, S. (1979a): Physical models for the analysis of acoustical systems in biology. Quart. Rev. Biophysics 12, 25–65.

Fletcher, N.H. and Thwaites, S. (1979b): Acoustical analysis of the auditory system of the cricket *Teleogryllus commodus* (Walker). J. Acoust. Soc. Am. 66, 350–357.

Hermes, D.J., Aertsen, A.M.H.J., Johannesma, P.I.M. and Eggermont, J.J. (1981): Spectro-temporal characteristics of single units in the auditory midbrain of the lightly anaesthetised grassfrog (*Rana temporaria* L.) investigated with noise stimuli. Hearing Res. 5, 145–179.

Hetherington, T.E. and Lombard, R.E. (1982): Biophysics of underwater hearing in anuran amphibians. J. Exp. Biol. 98, 49–66.

Hill, K.G., Lewis, D.B., Hutchings, M.E. and Coles, R.B. (1980): Directional hearing in the Japanese quail (*Coturnix c. japonica*) I. Acoustic properties of the auditory system. J. Exp. Biol. 86, 131–151.

Kleindienst, H.U., Koch, U.T. and Wohlers, D.W. (1981): Analysis of the cricket auditory system by acoustic stimulation using a closed sound field. J. Comp. Physiol. 141, 283–296.

Liff, H. (1969): Responses from single units in the eighth nerve of the leopard frog. J. Acoust. Soc. Am. 45, 512–513.

Lombard, R.E. and Straughan, I.R. (1974): Functional aspects of anuran middle ear structures. J. Exp. Biol. 61, 71–93.

Lombard, R.E., Fay, R.R. and Werner, Y.L. (1981): Underwater hearing in the frog. J. Exp. Biol. 91, 57–71.

Moffat, A.J.M. and Capranica, R.R. (1978): Middle ear sensitivity in anurans and reptiles measured by light scattering spectroscopy. J. Comp. Physiol. 127, 97–107.

Olson, H.F. (1958): Dynamical Analogies. Van Nostrand, Princeton, NJ.

Palmer, A.R. and Pinder, A.C. (1984): The directionality of the frog ear described by a mechanical model. J. Theor. Biol. 110, 205–215.

Paton, J.A., Capranica, R.R., Dragsten, P.R. and Webb, W.W. (1977): Physical basis for auditory frequency analysis in field crickets. J. Comp. Physiol. 119, 221–240.

Pinder, A.C. and Palmer, A.R. (1983): Mechanical properties of the frog ear: vibration measurements under free- and closed-field acoustic conditions. Proc. R. Soc. London Ser. B 219, 371–396.

Rheinländer, J., Gerhardt, H.C., Yager, D.D. and Capranica, R.R. (1979): Accuracy of phonotaxis by the green treefrog (*Hyla cinerea*). J. Comp. Physiol. 133, 247–255.

Rheinländer, J., Walkowiak, W. and Gerhardt, H.C. (1981): Directional hearing in the green treefrog: a variable mechanism? Naturwissenschaften 68, 430–431.

Rosowski, J.J. and Saunders, J.C. (1980): Sound transmission through the avian interaural pathways. J. Comp. Physiol. 136, 183–190.

Strother, W.F. (1959): The electrical activity of the auditory mechanism in the bullfrog (*Rana catesbeiana*). J. Comp. Physiol. Psychol. 52, 157–162.

Vlaming, M.S.M.G., Aertsen, A.M.H.J. and Epping, W.J.M. (1984): Directional hearing in the grassfrog (*Rana temporaria* L.) I. Mechanical vibrations of tympanic membrane. Hearing Res. 14, 191–201.

Wilczynski, W., Resler, C. and Capranica, R.R. (1981): A study of the mechanism underlying the directional sensitivity of the anuran ear. Soc. Neurosci. 7, Abstr. 4g.5.

Wilczynski, W., Resler, C. and Capranica, R.R. (1982): Relative sensitivity of tympanic and extratympanic sound transmission in the leopard frog, *Rana pipiens*. Soc. Neurosci. 8, Abstr. 270.6.